P4.7 An Investigation of Mesoscale Convective Systems Crossing the Appalachian Mountains

Casey E. Letkewicz* and Matthew D. Parker
North Carolina State University, Raleigh, North Carolina

1. INTRODUCTION

Mesoscale convective systems (MCSs) have been the subject of numerous observational and numerical modeling studies, many of which have focused on those occurring in the central United States. While large strides have been made in the understanding of these systems, the interaction of MCSs with terrain is a subject which has only just recently emerged (Frame and Markowski 2006; Keighton et al. 2007).

In the eastern portion of the United States, the forecasting of MCSs is complicated by the influence of the Appalachian Mountains. At times these systems are able to cross the terrain, often producing severe weather in the lee of the Appalachians. Other times, MCSs instead dissipate upon entering the mountains. Keighton et al. (2007) recently conducted a study which examined these systems in more detail, finding that the ability of an MCS to cross the Appalachians was strongly dependent upon diurnal heating. Most cases categorized as "noncrossing" reached the western slopes or dissipated to the west during the overnight and early morning hours while "crossing" cases tended to encounter the terrain during peak heating. Frame and Markowski (2006) examined these storms in an idealized framework, and found that squall lines traversing terrain went through a cycle of orographic enhancement on the upslope side, weakening, and subsequent restrengthening as the cool outflow air pooled at the base of the mountain downstream to form a hydraulic jump.

In light of these past studies, there still exists a need to differentiate crossing and noncrossing environments and determine what other key processes may be at work. The hope is that this study can aid forecasters in identifying typical environments of each case type and serve as a guide to understanding these systems better. This is accomplished through analysis of observations as well as idealized simulations to understand the key processes at work in these systems.

Section 2 will discuss the data and methodology of this study; section 3 will discuss the observational and preliminary modeling results; finally, section 4 will conclude and highlight ongoing work.

* *Corresponding author address:* Casey E. Letkewicz, Department of Marine, Earth, & Atmospheric Sciences, North Carolina State University, Campus Box 8208, Raleigh, NC 27695–8208. E-mail: celetkew@ncsu.edu

2. DATA AND METHODOLOGY

a. *Observations*

A random sampling of 20 crossing and 20 noncrossing cases were chosen from the Keighton et al. (2007) database of MCSs in the Appalachian region. These systems were categorized based on whether or not they were able to produce severe weather in the lee of the mountains. If an MCS produced severe weather reports on the eastern side of the barrier, it was categorized as "crossing." Those which did not produce severe weather reports in the lee were categorized as "not crossing." Noncrossing events also typically did not survive for long as non-severe convection east of the mountains. For further detail on how the events were categorized, please see Keighton et al. (2007).

To more closely analyze the environments of these cases, two soundings were chosen for each case: one to represent the upstream environment west of the mountains and one to represent the downstream environment east of the barrier. The soundings were chosen so that they approximately represented the inflow environment. This determination was difficult at times due to the limitations of the data; however, suitable soundings were found for each case. Each sounding was also modified with the surface conditions within an hour before the MCS passed through, in order to obtain as accurate a representation of the inflow environment as possible.

After modifying the soundings, numerous parameters were calculated and averaged to represent the thermodynamic and kinematic environment for the cases. A complete listing of the parameters used for this study, including those deemed important for MCS maintenance by Coniglio et al. (2007), can be found in the Appendix.

In order to determine the extent to which crossing and noncrossing environments were different, statistical analysis was performed. The Monte Carlo method was used to obtain "p-values" which represent the probabil-

ity that the difference between groups is due to random sampling.

b. *Model Design*

This study also utilized 3D simulations of idealized squall lines, employing Version 1.11 of the Bryan Cloud Model (CM1), a three-dimensional nonhydrostatic numerical model (Bryan and Fritsch 2002). A horizontal gridspacing of 1 km and a vertical grid stretched from 150 m at the model surface to 500 m aloft was used. The periodic y-dimension was 60 km in extent; the across-line x-dimension was nominally 600 km, although this was increased for the faster-moving squall line simulations.

Convection was initiated using a line thermal with a θ' of +4 K and the idealized Weisman and Klemp (1982) thermodynamic profile. The squall line was allowed to evolve and mature for three hours before its cold pool reached the base of the mountain. The dimensions of the mountain remained constant, a Gaussian bell-shaped hill with a half width of 50 km and a height of 1 km, roughly approximating the dimensions of the Appalachian Mountains. The mountain was infinitely long in the y-direction.

Observational results (discussed in section 3a) motivated the focus of model tests on the wind profile. Profiles utilized are illustrated in Figure 1. Two profile types were employed: the idealized Rotunno et al. (1988) wind profile (serving as the control, and increased or decreased by 5 m/s) and composite observed wind profiles from the downstream environment (one representing the crossing cases and one for the noncrossing cases). Each change in the shape of the wind profile was additionally accompanied by a simulation which removed the terrain for comparison.

3. RESULTS

a. *Observations*

Though numerous parameters were used to determine the thermodynamic and kinematic environment of the MCSs in this study, only a few stand out as being useful in differentiating between crossing and noncrossing cases. Tables 1 and 2 rank the upstream and downstream parameters based on their discriminatory power (only parameters with a p-value less than 0.4 are shown). Comparison of these tables reveals that the downstream environment was a much better indicator of whether or not an MCS would cross, as there are several parameters with a very low (less than 0.05) p-value, while only one upstream parameter had a p-value less than 0.05. This simple comparison shows that the environment that the MCS is moving into is more important for its maintenance than the one in which it developed. However, DCAPE was found to be the parameter which best separates case types in the upstream environment. Crossing cases on average contained higher amounts of DCAPE than noncrossing cases, and this finding can be associated with the potential for stronger cold pools (more evaporational cooling).

Many of the discriminatory downstream parameters are linked to the stability of the environment. Notably, the downstream environment tended to be quite a bit more unstable for crossing than noncrossing cases, with nearly 2000 J/kg more CAPE for the surface-based and most unstable parcels. This result is consistent with Keighton et al. (2007)'s finding that most crossing cases occur during the peak of daytime heating (i.e. when there is the greatest amount of instability). Crossing cases also tended to have higher surface potential and equivalent potential temperatures and mixing ratios, which coincide with greater instability. The surface to 500 mb θ_e difference's significance is mainly attributable to the surface θ_e value, which was also a discriminatory parameter. Additionally, the low level lapse rate was greater for crossers. Finally, the averaged MUCIN was smaller (less inhibition) for crossing cases than for noncrossing cases. It is important to note that many of these parameters are correlated with one another, thus the key finding is that crossers tended to have a thermodynamic environment which was more favorable for convection.

The other primary category of downstream parameters which best separated crossing and noncrossing MCS environments is wind and shear. The most useful parameters included maximum bulk shear, 0-3 km shear, 3-12 mean wind speed, 0-6 km shear, and the mountain-perpendicular component of the 0-3 km shear and the mean 3-12 km wind speed. Interestingly, the average for each of these parameters was *smaller* for crossers than noncrossers. Higher shear is generally beneficial (to an extent) for MCS maintenance (Rotunno et al. 1988, Coniglio et al. 2007), thus it is perplexing to find the opposite observed. We wondered if crossing cases tended to dominate in the warm season, which climatologically has weaker shear due to less baroclinicity. Yet, a sample comparison of shears between case types reveals that the trend is *not* dependent on the time of year (Figure 2). It has been observed anecdotally and noted in an idealized setting (Frame and Markowski 2006) that MCSs weaken while traversing the barrier, in part because the cold pool is weakened or partially blocked. Thus, it may be that smaller shear values downstream provide a better balance with a weaker cold pool (i.e. weaker baroclinic vorticity generated from the cold pool balanced with the weaker vorticity from the environmental shear; Rotunno et al. 1988). The finding that crossing cases had

a weaker mean wind could be explained by considering slope flows induced by the ambient wind. In a westerly wind regime, upslope flow is located on the windward side of the mountain, while downslope flow is found in the lee. This sinking motion on the eastern side can act to suppress convection, thus it can be benefical for squall lines to have a weaker mean wind so that this suppression is not as strong.

b. *Simulations*

In light of the unexpected observation of comparatively weaker shear and mean wind in crossing cases, we now further evaluate their unique role through idealized model simulations. The first set of sensitivity tests dealt with changing the mean wind of an idealized wind profile like that employed by Rotunno et al. (1988). The mean wind was then alternately increased and decreased by adding a constant to this profile (Figure 1). In a run with no terrain, increasing or decreasing the mean wind should simply create a faster or slower moving MCS of similar evolution. However, when terrain is included, slope flows come into play.

The control and increased mean wind run are similar in that they both appear to uphold the Frame and Markowski (2006) conceptual model, where there appears to be slightly enhanced reflectivity on the upslope side of the mountain, subsequent weakening, and then redevelopment on the downstream side (Figure 3). Hovmoller diagrams of along-line averaged surface vertical velocity also reveal their similarity, illustrating comparable slope flow structure but with slightly varying magnitudes (Figure 4). It is clear from Figure 4 that due to the westerly wind profile, positive vertical velocities (upslope) dominate on the western half of the mountain (potentially enhancing the convection), while negative vertical velocities (downslope) dominate on the eastern half. Once the MCS crosses the mountain peak, stronger sinking motion aids in the supression of convection.

The decreased mean wind run is less clear-cut, particularly due to the development of a new convective line out ahead of the original (Figure 3). We have observed such real-world behavior on a number of days, and further study is warranted. The environmental low level wind reversal may be the cause of this new convection, particularly due to the impacts slope flows and resultant vertical velocities. Figure 4 illustrates general sinking motion west of the mountain (potentially working to weaken the approaching convection) and rising motion east of the mountain. The result of this flow reversal and weaker mean wind is made clear by examining the strength of the cold pool, which is noticeably weaker than in the other simulations (Figure 5). Though unconventional, a crossing MCS was still produced despite its weaker cold pool and slower storm motion.

The next set of simulations incorporated a more realistic wind profile, based on the observed downstream mountain-perpendicular component of the total wind. The observed crossing wind profile simulation does indeed produce a crossing MCS which appears to go through a cycle of slight enhancement, weakening, and subsequent restrengthening (Figure 6). Notably, the reflectivity is much stronger in the eastern half of the domain when the mountain is present as compared to when there is no mountain. The noncrossing wind profile also produces an MCS which is able to traverse the barrier, though the reflectivity does appear to be weaker than the crossing profile simulation, particularly in the first couple of hours of the simulation and as well as downstream of the mountain after crossing has occurred.

Comparing the cold pool strengths of these observed profile simulations provides further insight (Figure 7). Without terrain, the noncrossing profile simulation produces a stronger cold pool than the crossing profile simulation. When terrain is added, both the crossing and noncrossing cold pools are weakened (as compared to their counterparts without terrain), yet the new cold pools are now of similar strength. This suggests that the noncrossing profile's cold pool is weakened *more* due to its interaction with the barrier, as it was initially stronger in the case without terrain. Meanwhile, the cold pool in the crossing profile simulation is less affected by its interaction with the barrier. This result, combined with the comparison of simulated reflectivity (i.e. crossing profile reflectivity is stronger in presence of terrain, whereas noncrossing profile reflectivity is slightly weaker with terrain), illustrates that the shape of the wind profile itself is also important in determining if an MCS will cross the mountains. Recall, however, that in the observed MCSs (Table 2), changes in the downstream instability also played a large role, an effect that is relatively straightforward, and thus is not taken into account in these simulations.

4. CONCLUSIONS & FUTURE WORK

A collection of 20 crossing and 20 noncrossing MCS cases in the Appalachian region served as the basis for this investigation. The downstream environment east of the mountains appears to be essential in determining whether crossing will occur. Specifically, higher amounts of instability, less shear, and a weaker mean wind best separated the observed data. While greater instability is not a surprising result, less shear and a weaker mean wind is. We hypothesize that the theory put forth by Rotunno et al. (1988) on the maintenance of squall lines may provide the reasoning behind the ob-

served weaker shear, while a weaker mean wind may be beneficial due to weaker downslope flow in the lee acting to suppress the convection.

We designed simulations utilizing the CM1 numerical model built upon the idealized results of Frame and Markowski (2006), seeking to isolate the impact of both idealized and observed wind profiles. Varying the mean wind of the idealized wind profile does not change the ability of the MCS to cross the terrain, though it does influence the convection produced. The increased mean wind simulation essentially produced a faster moving system similar to the control and still went through a period of orographic enhancement, weakening, and then restrengthening on the downstream side. The decreased mean wind run also produced a crossing MCS, but was unique in that a new line of convection developed out ahead of the original line, thus deviating from the Frame and Markowski (2006) conceptual model. A second set of simulations incorporating observed wind profiles into the model illustrated the importance of the shape of the wind profile, particularly since the MCS in the noncrossing wind profile had a less favorable interaction with terrain than that in the crossing wind profile.

Currently, we are working on simulations which vary the mean wind for the observed wind profiles, as well as performing sensitivity tests which change the amount of low level shear in the idealized wind profiles. Further analysis of the dynamics of these systems is also underway to strive for complete understanding.

Acknowledgements. The research reported here is supported by the National Science Foundation under Grant ATM-0552154 and by NOAA under grant NA07 NWS4680002. Thanks also go to the Convective Storms Group at NC State University for their assistance and feedback.

References

Bryan, G. H., and J. M. Fritsch, 2002: A benchmark simulation for moist nonhydrostatic numerical models. *Mon. Wea. Rev.*, **130**, 2917–2928.

Coniglio, M. C., H. E. Brooks, S. J. Weiss, and S. F. Corfidi, 2007: Forecasting the maintenance of quasi-linear mesoscale convective systems. *Wea. Forecasting*, **22**, 556–570.

Frame, J., and P. Markowski, 2006: The interaction of simulated squall lines with idealized mountain ridges. *Mon. Wea. Rev.*, **134**, 1919–1941.

Keighton, S., J. Jackson, J. Guyer, and J. Peters, 2007: A preliminary analysis of severe quasi-linear mesoscale convective systems crossing the appalachians. Preprints, *22nd Conf. on Weather Analysis and Forecasting*, Park City, UT, Amer. Meteor. Soc., 16 pp.

Rotunno, R., J. B. Klemp, and M. L. Weisman, 1988: A theory for strong, long–lived squall lines. *J. Atmos. Sci.*, **45**, 463–485.

Weisman, M. L., and J. B. Klemp, 1982: The dependence of numerically simulated convective storms on vertical wind shear and buoyancy. *Mon. Wea. Rev.*, **110**, 504–520.

Appendix

Parameters used for this study include Convective Available Potential Energy (CAPE) and Convective Inhibition (CIN) of the surface parcel, the most unstable parcel (MUCAPE & MUCIN), and the 0-1 km mixed layer parcel (MLCAPE & MLCIN); downdraft CAPE (DCAPE), LCL height, 0-1 km, 0-3 km, 0-6, 3-12 km, and maximum bulk shear (defined as the maximum shear between 0-1 km and 6-10 km); 1 km wind speed, 3-12 km mean wind speed, 0-3 and 3-8 km lapse rate, 850 mb dewpoint, θ, and θ_e; surface to 500 mb difference in θ_e, precipitable water, and surface properties such as θ, θ_e, and mixing ratios. Note that CIN values were only averaged if they were accompanied by CAPE values greater than zero. Each shear and wind variable was also calculated for the mountain-perpendicular component of the wind.

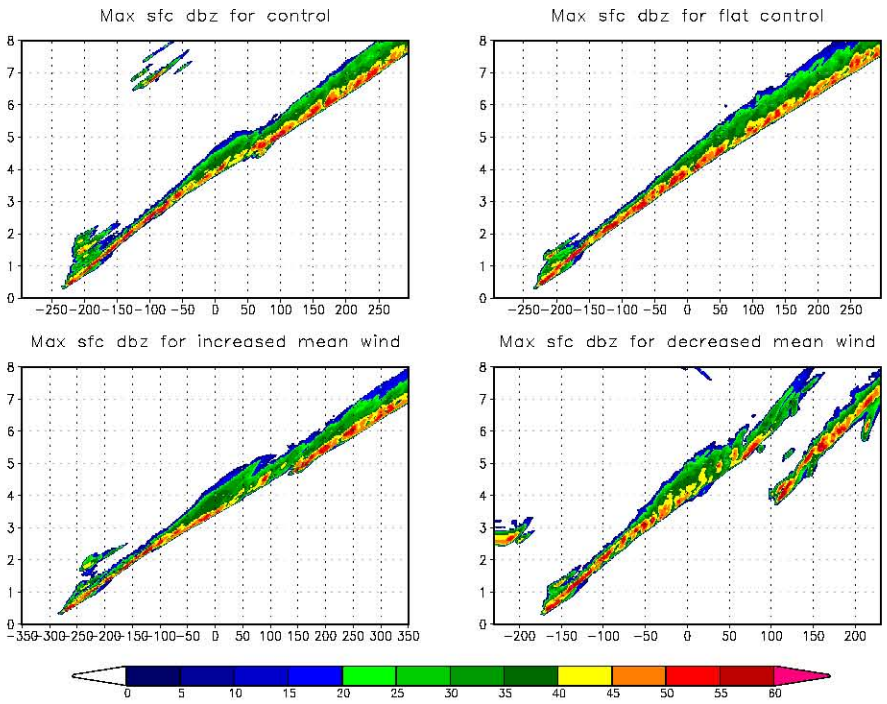

Figure 3: Hovmoller diagrams of maximum surface simulated reflectivity for the control, flat control, increased mean wind, and decreased mean wind simulations. Time in hours is the y-axis, and distance from the mountain peak (at x=0) in km is the x-axis.

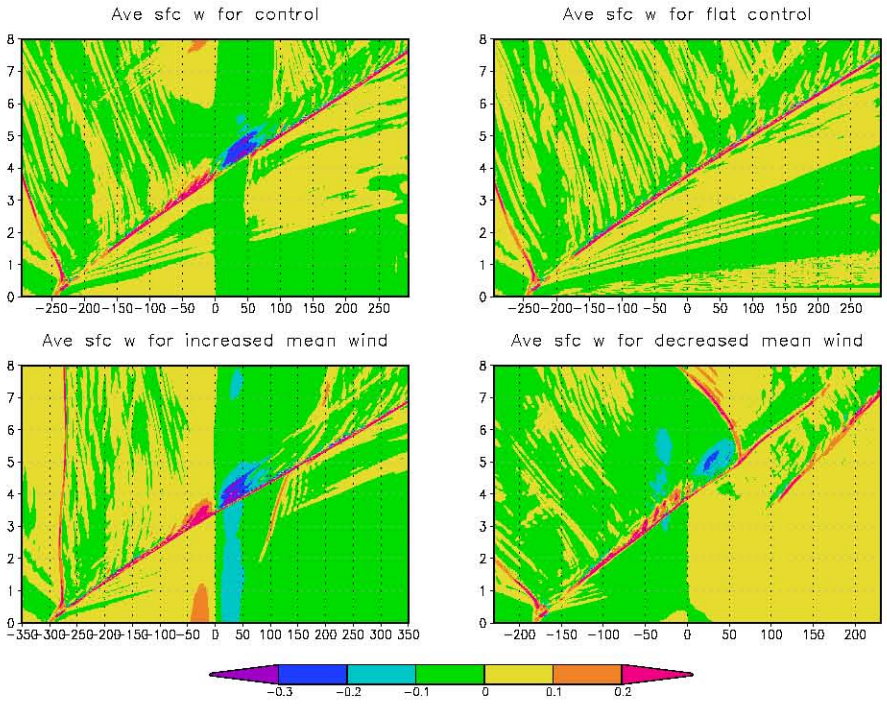

Figure 4: Hovmoller diagrams of line-averaged surface vertical velocity (in m/s) for the control, flat control, increased mean wind, and decreased mean wind simulations. Time in hours is the y-axis, and distance from the mountain peak (at x=0) in km is the x-axis.

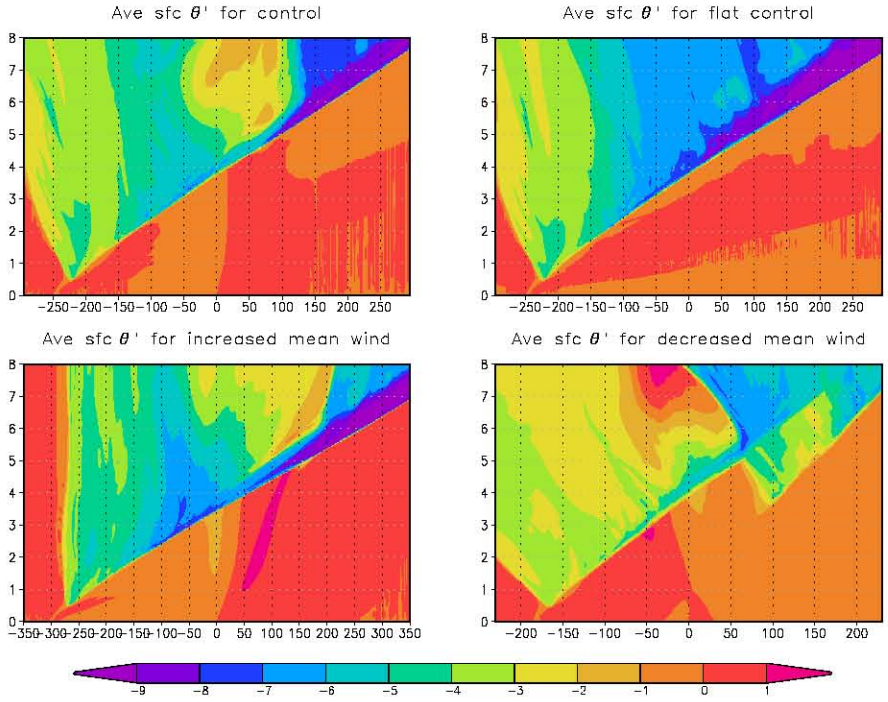

Figure 5: Hovmoller diagrams of line-averaged surface θ' (K) for the control, control flat, increased mean wind, and decreased mean wind simulations. Time in hours is the y-axis, and distance from the mountain peak (at x=0) in km is the x-axis.

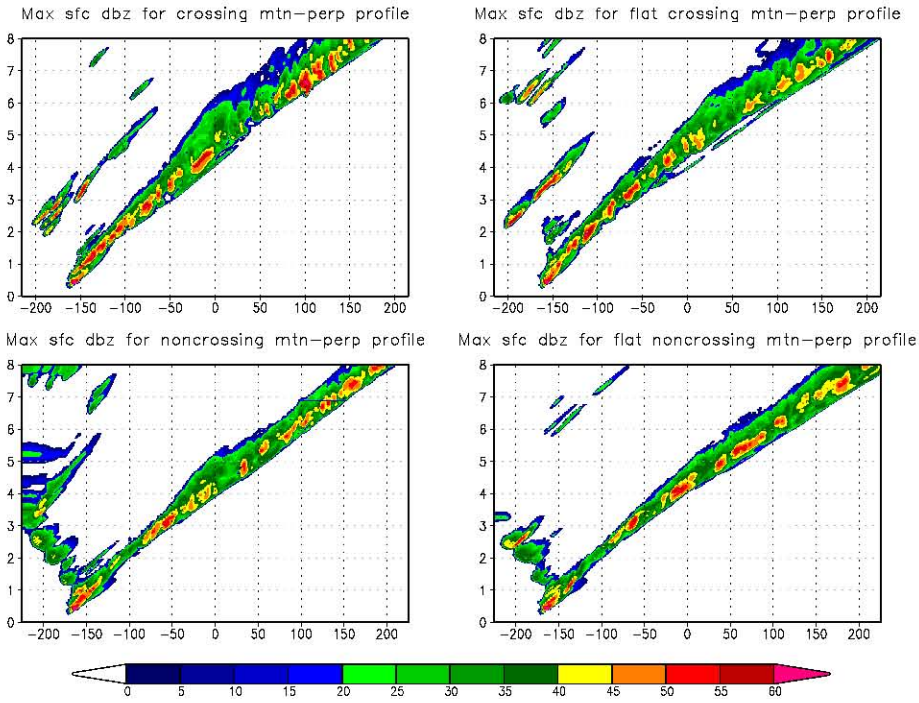

Figure 6: As in Fig. 3 but for the observed wind profile simulations.

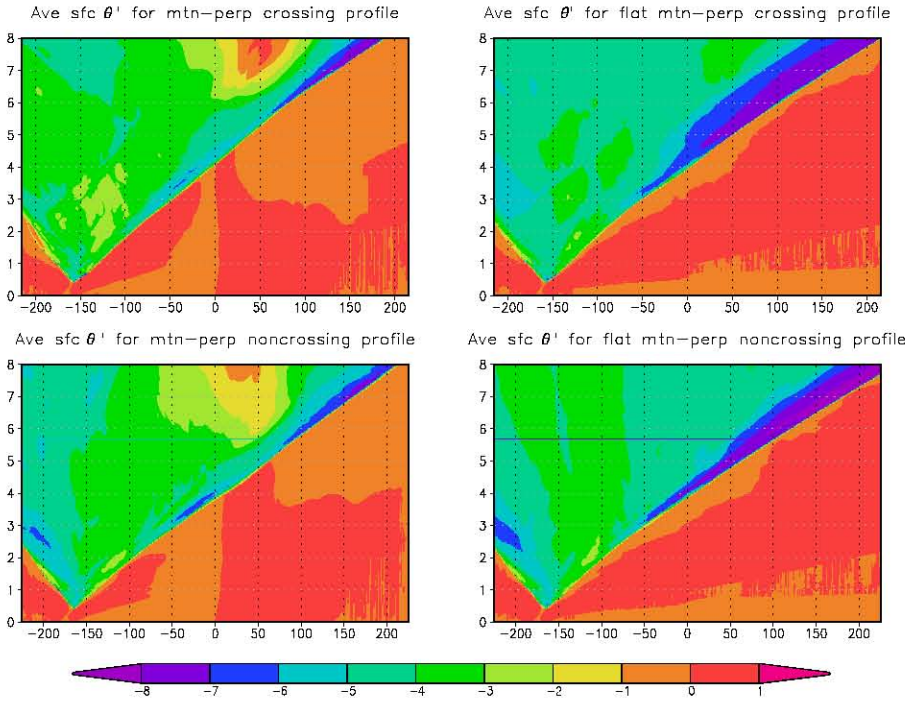

Figure 7: As in Fig. 5 but for the observed wind profile simulations

Parameter	Crossing Avg.	Noncrossing Avg.	p-value
DCAPE (J/kg)	-688.6	-509.6	0.024140
MUCIN (J/kg)	-7.4	-26.6	0.077949
Mtn-perpendicular 0-6 km Shear (m/s)	7.7	11.0	0.089889
Maximum Bulk Shear (m/s)	23.1	29.8	0.124039
MLCAPE (J/kg)	963.0	464.9	0.130819
0-3 km Shear (m/s)	11.7	14.8	0.136659
2-8 km Shear (m/s)	12.8	18.2	0.145909
0-1 km Shear (m/s)	9.4	12.0	0.156688
0-6 km Shear (m/s)	13.1	18.3	0.207448
1 km Wind Speed (m/s)	12.1	14.5	0.267787
850 mb θ_e (K)	336.8	332.3	0.271777
MUCAPE (J/kg)	2068.5	1437.9	0.285007
3-12 km Mean Wind Speed (m/s)	17.8	21.3	0.282637
850 mb Dewpoint (^{o}C)	12.7	11.1	0.302427
Mtn-perpendicular Maximum Bulk Shear (m/s)	15.7	19.4	0.303237
Mtn-perpendicular Mean 3-12 km Wind Speed (m/s)	11.2	13.5	0.34917
Mtn-perpendicular 0-1 km Shear (m/s)	6.1	6.9	0.389006

Table 1: Parameter averages and p-values for the upstream environment.

Parameter	Crossing Avg.	Noncrossing Avg.	p-value
SB CAPE (J/kg)	2403.9	518.9	0.000230
MUCAPE (J/kg)	2712.9	903.3	0.000260
Surface-500 mb θ_e Difference (K)	18.3	6.1	0.001410
0-3 km Lapse Rate (K/km)	7.0	5.5	0.002520
Maximum Bulk Shear (m/s)	20.1	30.2	0.003130
0-3 km Shear (m/s)	9.3	15.7	0.003170
3-12 km Mean Wind Speed (m/s)	12.8	21.1	0.003350
0-6 km Shear (m/s)	12.5	19.6	0.005140
Surface θ (K)	301.2	296.8	0.011200
Surface θ_e (K)	343.8	331.9	0.013150
LCL Height (m AGL)	866.2	521.5	0.017590
Mtn-perpendicular 0-3 km Shear (m/s)	5.7	9.3	0.018090
Surface Mixing Ratio (g/kg)	15.2	12.6	0.021470
Mtn-perpendicular Mean 3-12 km Wind Speed (m/s)	8.7	13.3	0.032580
MUCIN (J/kg)	-22.6	-62.8	0.046850
Mtn-perpendicular Maximum Bulk Shear (m/s)	13.9	19.4	0.055389
MLCAPE (J/kg)	593.8	317.7	0.056579
Mtn-perpendicular 0-6 km Shear (m/s)	8.5	11.6	0.100569
2-8 km Shear (m/s)	11.3	16.1	0.146079
SB CIN (J/kg)	-53.5	-104.1	0.228498
MLCIN (J/kg)	-69.2	-64.8	0.333607
850 mb Dewpoint (^{o}C)	11.4	10.1	0.354216

Table 2: Parameter averages and p-values for the downstream environment.